

Flux and fate of Yangtze River sediment delivered to the East China Sea

J.P. Liu ^{a,*}, K.H. Xu ^b, A.C. Li ^c, J.D. Milliman ^b, D.M. Velozzi ^a,
S.B. Xiao ^d, Z.S. Yang ^e

^a Department of Marine, Earth and Atmospheric Sciences, North Carolina State University, Raleigh, NC, 27695, USA

^b School of Marine Science, College of William and Mary, Gloucester Pt. VA 23062, USA

^c Institute of Oceanology, Chinese Academy of Sciences, Qingdao, 266071, China

^d South China Sea Institute of Oceanology, Chinese Academy of Sciences, Guangzhou, 510301, China

^e College of Geo-Marine Sciences, Ocean University of China, Qingdao 266003, China

Received 2 February 2005; received in revised form 22 April 2005; accepted 29 March 2006

Available online 8 September 2006

Abstract

Numerous cores and dating show the Yangtze River has accumulated about 1.16×10^{12} t sediment in its delta plain and proximal subaqueous delta during Holocene. High-resolution seismic profiling and coring in the southern East China Sea during 2003 and 2004 cruises has revealed an elongated (~ 800 km) distal subaqueous mud wedge extending from the Yangtze River mouth southward off the Zhejiang and Fujian coasts into the Taiwan Strait. Overlying what appears to be a transgressive sand layer, this distal clinoform thins offshore, from ~ 40 m thickness between the 20 and 30 m water depth to $< 1\text{--}2$ m between 60 and 90 m water depth, corresponding to an across shelf distance of less than 100 km. Total volume of this distal mud wedge is about 4.5×10^{11} m³, equivalent to $\sim 5.4 \times 10^{11}$ t of sediment. Most of the sediment in this mud wedge comes from the Yangtze River, with some input presumably coming from local smaller rivers. Thus, the total Yangtze-derived sediments accumulated in its deltaic system and East China Sea inner shelf have amounted to about 1.7×10^{12} t. Preliminary analyses suggest this longshore and across-shelf transported clinoform mainly formed in the past 7000 yrs after postglacial sea level reached its mid-Holocene highstand, and after re-intensification of the Chinese longshore current system. Sedimentation accumulation apparently increased around 2000 yrs BP, reflecting the evolution of the Yangtze estuary and increased land erosion due to human activities, such as farming and deforestation. The southward-flowing China Coastal Current, the northward-flowing Taiwan Warm Current, and the Kuroshio Current appear to have played critical roles in transporting and trapping most of Yangtze-derived materials in the inner shelf, and hence preventing the sediment escape into the deep ocean.

© 2006 Elsevier B.V. All rights reserved.

Keywords: East China Sea; Yangtze River; Clinoform; Delta; Mud wedge; Sea level

1. Introduction

Major rivers play a dominant role worldwide in transferring both particulate and dissolved materials

from the land to the coastal ocean. The total suspended sediment delivered by all rivers to the ocean is about 15×10^9 metric tons annually, of which Asian rivers discharge nearly more than 70% (Milliman and Meade, 1983; Milliman and Syvitski, 1992; Syvitski et al., 2005). Most of these sediments, however, are trapped in estuaries or deposited on adjacent continental shelves;

* Corresponding author.

E-mail address: jpliu@ncsu.edu (J.P. Liu).

only less than 5–10% of the fluvial sediments presently reach the deep sea (e.g. Meade, 1996). The river-dominated ocean margins also play a significant role in global biogeochemical cycles (Chen et al., 2003a,b; Cai and Dai, 2004; Dagg et al., 2004; McKee et al., 2004). The study of estuaries, deltas, and inner continental shelves, therefore has particular relevance as we seek to understand the link between present-day terrestrial processes and coastal marine deposition.

One of the best examples of the river-dominated ocean margins is the epicontinental shelf of the East China Sea, which together with the Yellow and Bohai seas, forms a contiguous shelf of about $0.75 \times 10^{12} \text{ m}^2$ in

area (Fig. 1). This wide and shallow shelf receives a large amount of terrigenous materials from two of the largest rivers in the world, the Yellow and Yangtze rivers. The Yellow River alone has discharged totally near 1.63×10^{12} tons sediment to the Bohai and Yellow seas during the past 10 kyr (Liu et al., 2002, 2004). The modern Yangtze River's annual sediment load has been about 480 million tons historically. When combined with the adjacent Yellow River (about 1 billion tons), the total equals $\sim 10\%$ of the global riverine sediment flux to the ocean (Milliman and Meade, 1983).

The Yangtze River originates from the Qinghai-Tibetan Plateau at an elevation of 6600 m, flowing

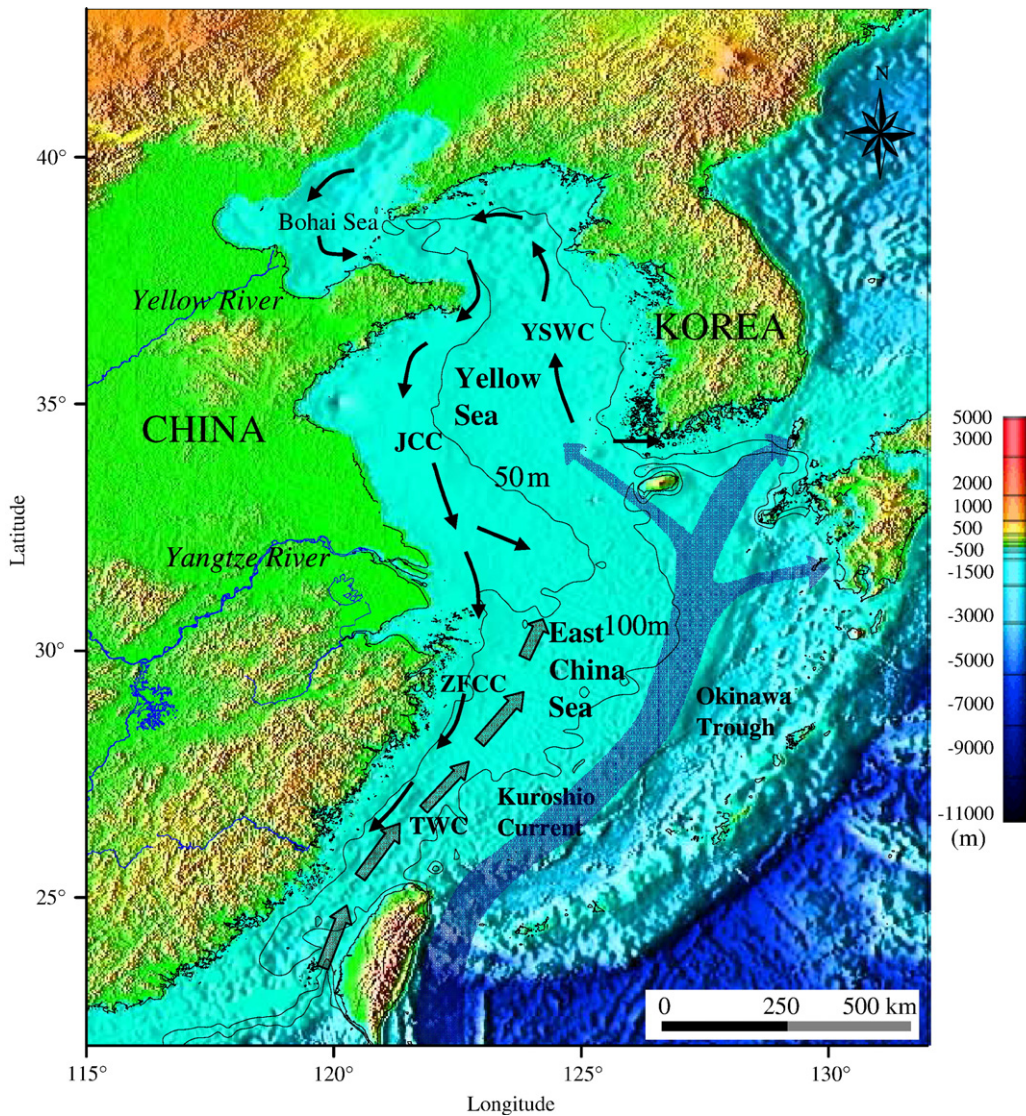


Fig. 1. Bathymetry and regional ocean circulation pattern in the East China Sea and Yellow Sea. JCC (Jiangsu Coastal Current); TWC (Taiwan Warm Current); YSWC (Yellow Sea Warm Current); ZFCC (Zhejiang Fujian Coastal Current).

eastward for more than 6300 km. This river drains an area of more than 1.94×10^6 km² before finally discharging into the East China Sea. It is the largest river in Asia in term of water discharge and third longest river in the world (Milliman and Meade, 1983). The modern Yangtze River discharges most of its annual sediment load between June and September, and short-term monthly deposition rates near the river mouth during this period are about 4.4 cm, in contrast to long-term accumulation rates, which are an order of magnitude less, ~ 1 –6 cm/yr (McKee et al., 1983; DeMaster et al., 1985; Chen et al., 2004). This difference between short- and long-term accumulation rates suggests that a major portion of the river-derived sediment is eroded periodically and is transported elsewhere, presumably southward to the Zhejiang and Fujian Provinces. This is commonly referred to as the “mud belt deposit on the inner shelf of the East China Sea” (Fig. 2), based on seafloor surficial sediments analysis (Qin, 1979; Qin et al., 1987).

A large number of geological and geophysical studies have been undertaken to examine fate of the Yangtze-derived mud deposit at the river mouth and inner shelf (Nittrouer et al., 1984; Butenko et al., 1985; DeMaster et al., 1985; Milliman et al., 1985, 1989; Chen et al., 1997, 2000; Li et al., 2000, 2001; Hori et al., 2001, 2002; Chen et al., 2003a,b). Over the last decade substantial research work has also been conducted on

the middle and outer shelves, including the north and south Okinawa Trough (e.g. Bartek and Wellner, 1995; Liu, 1997; Saito et al., 1998; Liu et al., 2000; Berne et al., 2002; Tsunogai et al., 2003; Liu et al., 2003). In addition, recent box-coring and geochemical analysis in the East China Sea has revealed that the sediment disperses longshore from the river mouth to the south, and is largely confined to the inner shelf (Huh and Su, 1999; Lin et al., 2002; Su and Huh, 2002).

Like other large rivers, the Yangtze also discharges substantial amounts of organic and inorganic carbon to the marginal sea, however, a large portion of these biogeochemically important materials is buried together with the rapid mud accumulation. Thus, the East China Sea has been found to be a sink rather than a source of global atmospheric CO₂ (Chen and Wang, 1999a,b; Liu et al., 2003; Tsunogai et al., 2003; Cai and Dai, 2004). The study of the history of Yangtze-derived sediment dispersal and deposition therefore may help us understand more thoroughly the relevant biogeochemical processes such as the carbon cycle.

However, until recently we still have little knowledge of the distribution, thickness, and sedimentary processes of Yangtze-derived sediments on the inner shelf of the East China Sea. Our knowledge is limited primarily to the surface sediment distribution along the Zhejiang and Fujian coasts (Fig. 2). The present study

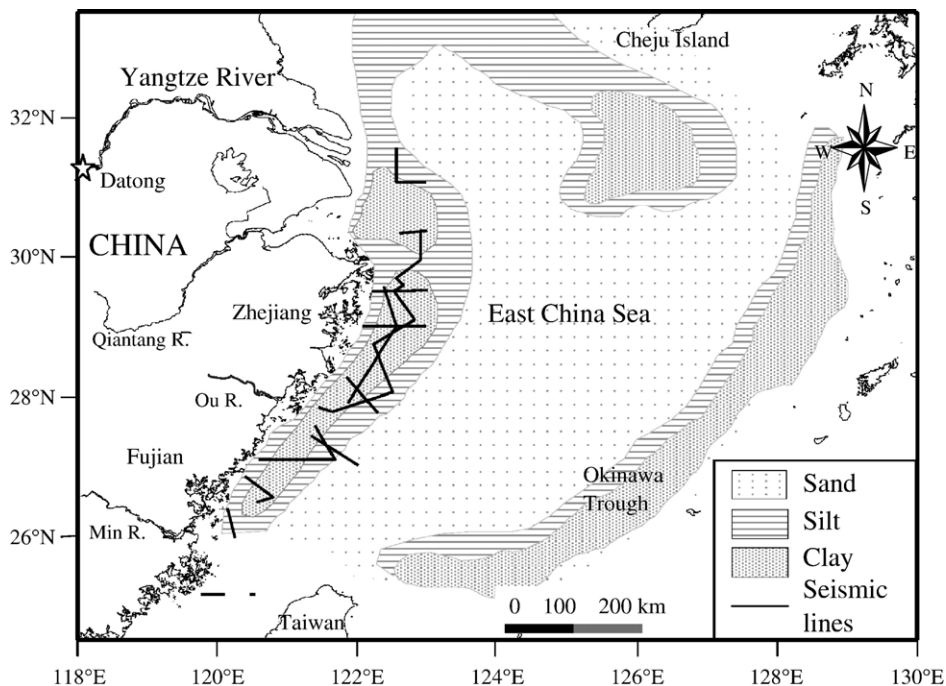


Fig. 2. Distribution of surface sediments in the East China Sea and Okinawa Trough (modified after Qin et al., 1987). Black lines are seismic track lines conducted in 2003 and 2004 in the inner shelf.

documents the nature of the innermost shelf of the East China Sea using high-resolution Chirp sonar profiles and sediment cores, with particular focus on the fate and depositional history of the Yangtze-derived sediment.

2. Study area

The modern Yangtze estuary is a large river and tide dominated depositional basin, located northwestern East China Sea with a mean tidal range of 2.7 m, and a maximum of 4.7 m. The average tidal current is about 1.0 ms^{-1} , that can reach more than 2.0 during spring tide (Chen et al., 1988). Over 100-yr data collected at the Datong Hydrological Gauging Station (see location in Fig. 2) show that the annual fresh water discharge to the Yangtze estuary can be as high as $9 \times 10^{11} \text{ m}^3$. However, the annual tidal prism from the sea into the estuary has a total volume of $84 \times 10^{11} \text{ m}^3$, which is an order of magnitude greater than the annual runoff (Chen et al., 1988, 2001). Thus the dispersal pattern of the Yangtze-derived sediment has been influenced strongly by the local semi-diurnal tidal cycles.

The warm and salty Kuroshio Current flows northward along the East China Sea shelf break (Fig. 1). As a result of this flow, the Taiwan Warm Current (TWC) and the Yellow Sea Warm Current (YSWC) give rise to a counterclockwise circulation in the East China Sea and Yellow Sea, with a relatively cold and brackish counter current — the China Coastal Current (CCC), which includes the Jiangsu Coastal Current (JCC) in the north and the Zhejiang–Fujian Coastal Current (ZFCC) in the south (Fig. 1) — flowing southward along the Chinese coast. This current intensifies in the winter, carrying the Yangtze's brackish water and sediment discharge southward along the inner shelf. Offshore, there is a northward flow of warm and saline middle-deep water flow, the TWC (Fig. 1). In summer, under the prevailing southeast monsoon, the northward TWC intensifies and, correspondingly, the southward ZFCC weakens (Beardsley et al., 1985; Lee and Chao, 2003).

The Holocene Yangtze delta covers an area of approximately $52,000 \text{ km}^2$, with $23,000 \text{ km}^2$ subaerial and $29,000 \text{ km}^2$ subaqueous (Li et al., 1986). The topography of the Yangtze delta plain is characterized mainly by an elevation of $\sim 2 \text{ m}$ above mean sea level in the central delta plain, rising to 3–5 m on the periphery of delta plain (Chen and Wang, 1999a,b). Numerous shallow cores and dating show that, the modern Yangtze delta has begun accreting after the postglacial sea level reached its mid-Holocene highstand ~ 7000 yrs ago (Yan

and Hong, 1987; Chen and Stanley, 1993; Stanley and Warne, 1994; Li et al., 2000, 2003). Over the past 3000 yrs the high sea-level stand has gradually retreated, approaching its present level (Yang and Xie, 1984; Yan and Hong, 1987; Zhao et al., 1994). Deceleration of sea-level rise by mid-Holocene time induced fluvial sediments to accumulate along the periphery of the delta plain (Stanley and Chen, 1996).

Close to the Yangtze River's mouth, in the subaqueous delta, four sedimentary facies (A–D) have been defined (Chen et al., 2000). Facies A, delta front — fine sand and silt facies; Facies B, prodelta — silty clay and clayey silt facies with abundant burrowing and rich in organic matter; Facies C, prodelta to continental shelf — sand–silt–clay facies, with thin layers of sand and clay interbedded and highly-laminated muds of storm deposition (Wang et al., 2006-this volume), and Facies D, late Pleistocene relict sands facies, mixed with shell fragments. From bottom upward, the late Quaternary stratigraphy of the deltaic deposit consists of late Pleistocene terrigenous (fluvial and lacustrine), Holocene transgressive silt, prodelta clay and delta front fine sand and silt. Due to the high sedimentation rate and limited bio-benthic activities, the inner-shelf mud deposit is generally laminated, with only

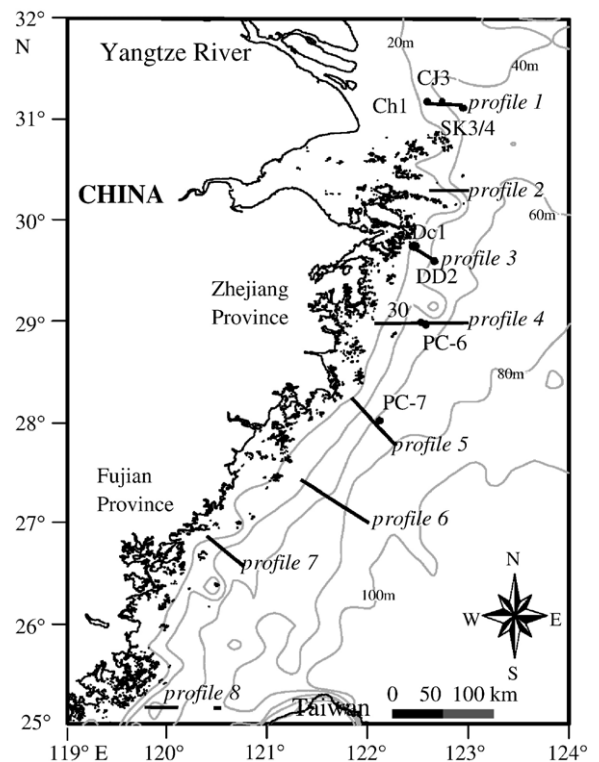


Fig. 3. Selected seismic lines from 2003 and 2004 surveys and cores discussed in this paper.

minor evidence of burrowing (Nittrouer et al., 1984; Wang et al., 2006-this volume).

3. Methods and data

In order to document the distribution and thickness of the Yangtze-derived mud, two geological and geophysical investigations were conducted in September 2003 and May 2004, (Figs. 2, 3). A high-resolution EdgeTech 0512i Chirp Sonar Sub-bottom Profiler (frequency range: 0.5–12 k) was used to obtain more than 1200 km seismic data. All seismic sub-bottom profiles were post-processed using the Discover software; an acoustic velocity of 1500 ms^{-1} was assumed to calculate water depth and sediment thickness (cf. Chen and Stanley, 1993; Chen et al., 2003a,b). A grab sampler obtained surface sediment samples, and gravity and box

corers collected shallow cores. Grain-size analysis was done with a Cilas Laser Particle Size Analyzer (model: 940 L).

Eight of 25 seismic profiles are discussed in this paper (Fig. 3). In addition to published ^{14}C dating, 11 new ages were obtained by testing foraminifera fossils from cores DD2, 30 and PC-6 dated at the NOSAMS lab of the Woods Hole Oceanographic Institution. Radiocarbon ages are reported in calendar year (BP) calibrated using Calib4.3 (Stuiver et al., 1998).

The inner shelf and Zhejiang Fujian mud wedge thickness was determined using the newly acquired seismic data. Sixteen piston cores collected by Lan et al. (1993) in the Taiwan Strait were used to define the southernmost boundary of the mud wedge. Sediment volume was calculated using software Surfer. Thickness of the Yangtze-derived mud on the delta plain, and in the

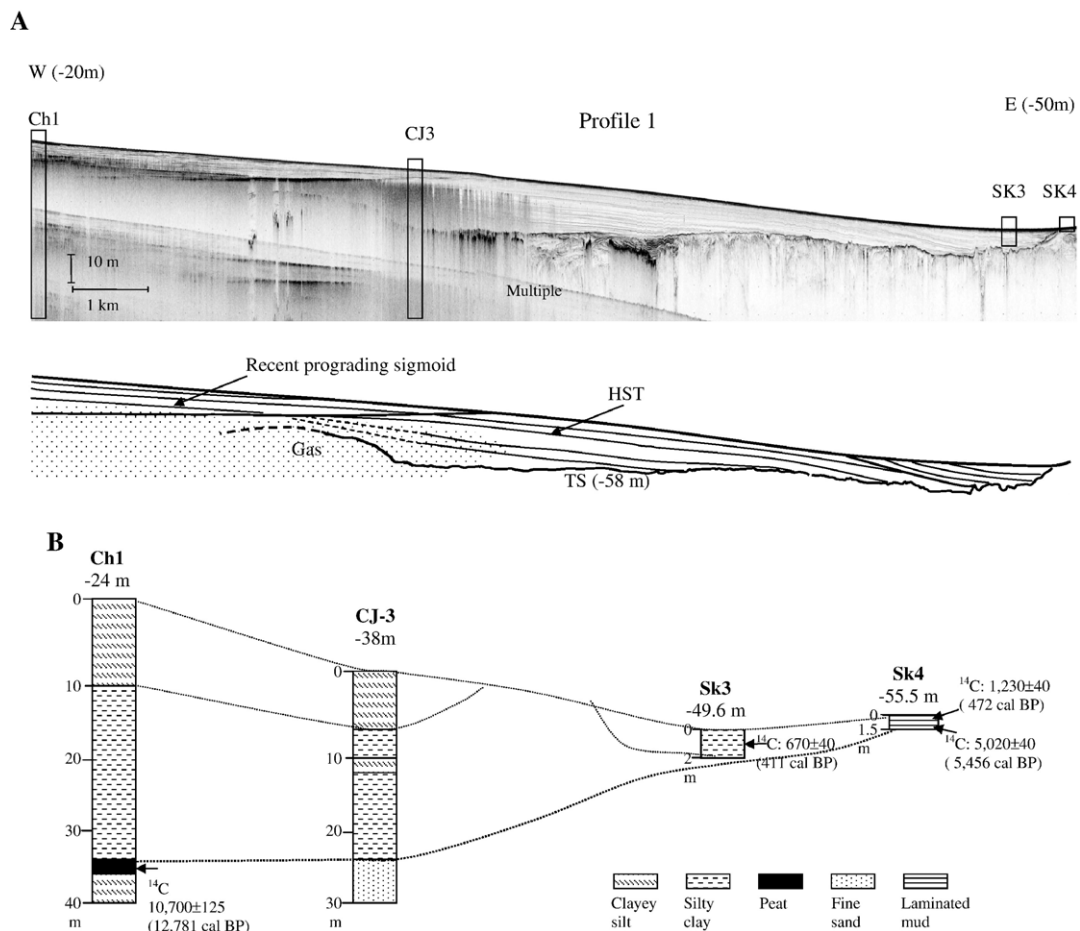


Fig. 4. (A) Seismic profile 1 located at the Yangtze subaqueous delta, which shows seaward (eastward) progradation of the clinoform (HST) overlying on the uneven TS. (B) Cores show the age of the TS and overlying deposits. Ch1 is from Qin et al. (1987), CJ-3 from (Chen et al., 2000), and SK-3 and SK-4 from (Wang et al., 2005). Location of profile and cores is shown in Fig. 3.

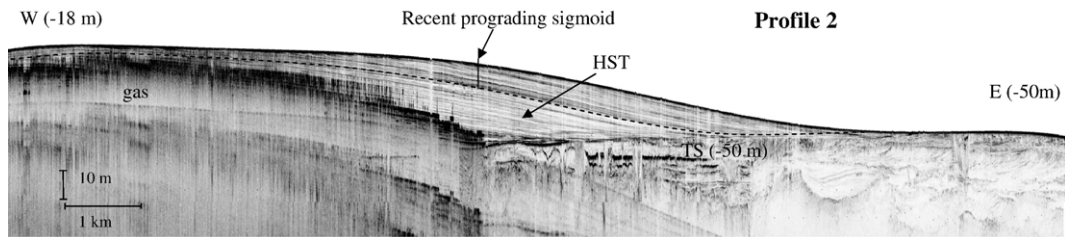


Fig. 5. Seismic profile 2 located at the outside Hangzhou Bay, showing the mud wedge and the easternmost boundary of the clinoform. Location of profile is shown in Fig. 3.

estuary and adjacent subaqueous delta was based on earlier studies by Chen and Stanley (1993), and Li C. et al. (2000, 2001, 2002) and Li et al. (2003).

4. Results and analyses

Seismic profiles reveal an extensive clinoform extending southward from the Yangtze estuary down along the Zhejiang and Fujian provinces, nearly 800 km into the middle of Taiwan Strait (Figs. 3–11). Thickest accumulation (~40 m) is between the 20–30 m isobaths, and the clinoform thins offshore, pinching out at water depths 60 to 70 m, less than 100 km from land. The high-resolution seismic profiles allow more closely examination of the internal architecture and depositional history of the Yangtze mud wedge.

4.1. Transgressive surface, deposits and maximum flooding surface

Overall, seismic profiles show a prominent subsurface reflector, overlain by a thick clinoform that thins offshore (Figs. 4–11). Compared with previous geological and geophysical records from the Yangtze subaqueous delta (Chen et al., 2000) and other similar deltaic deposits off the Yellow River (Liu et al., 2004) and Po River (Cattaneo et al., 2003), this prominent acoustic reflector appears to be the base of the post-glacial transgressive surface (TS), which was apparently caused by a rapid landward transgression during a rapid sea-level rise (Liu et al., 2004). Below the TS, relict sands were observed in cores C3J, Dc1, DD2 and PC-6 (Figs. 4, 6, 7), basal peat deposits occurred in Ch1 (Fig. 4), or re-filled channel deposits (Figs. 4, 6–8).

In some profiles, above the TS, there is a subparallel transparent layer (Figs. 7–9) that is covered by progradational clinoform deposits. This thin basal mud deposit represents a transgressive system tract (TST) (Cattaneo et al., 2003; Liu et al., 2004), which formed before sea level reached its highstand. Close inspection of seismic profiles in Figs. 8–10 suggests that, the TST

is not only well-preserved beneath the mud wedge, but extends offshore and pinches out at water depths of 70–90 m (Fig. 9). This allows us to penetrate the entire sequence with short gravity cores, for instance, the core DD2 in profile 3 (Fig. 6) and PC-6 in profile 4 (Fig. 7). Both cores have a depositional unconformity where the young strata (<2 ka BP) prograde seaward and overlie directly strata older than 5 ka BP.

Above the TST, the clinoform progrades across shelf to 60–80 m water depth, where it downlaps directly onto the TST, separated by the maximum flooding surface (MFS) (see Figs. 7–9). AMS ^{14}C dates in core DD2, PC-6 and PC-7 indicate that most likely this MFS was formed slightly before 7 ka BP, which coincides with the middle Holocene highstand (Chen and Stanley, 1993; Stanley and Warne, 1994; Li et al., 2000, 2001, 2002, 2003).

It should be noted that the TST in the East China Sea is generally thin, less than 2 m, (Figs. 7–9). This suggests that sea level rose quickly and insufficient sediment was contributed (or at least accumulated) in this part of the ECS shelf during the last transgression.

4.2. Clinoform and highstand system tract

Above the TS or MFS, a prominent clinoform, locally 20–40 m in thickness, thins offshore to the east. The thick package of sediment deposited between the MFS and maximum relative sea-level highstand is termed highstand system tract (HST). Close inspection of many of the clinoform profiles shows a rather complex inner structure — which suggests there is at least two distinct sigmoidal units in this HST. Good examples can be seen in profiles 1, 5 and 8 (Figs. 4, 8, 11), where the uppermost sigmoid layer has not yet covered the earlier HST.

The lower part of the landward clinoform tends to be acoustically opaque (Figs. 4–7), presumably from biogenic gas (Diaz et al., 1996; Nittrouer et al., 1996; Liu et al., 2004), which in this case probably comes from basal peat deposits (Liu et al., 2002, 2004).

AMS ^{14}C dates in the cores DD2, 30, PC-6, and PC-7 suggest the HST began accumulating around 7 ka BP,

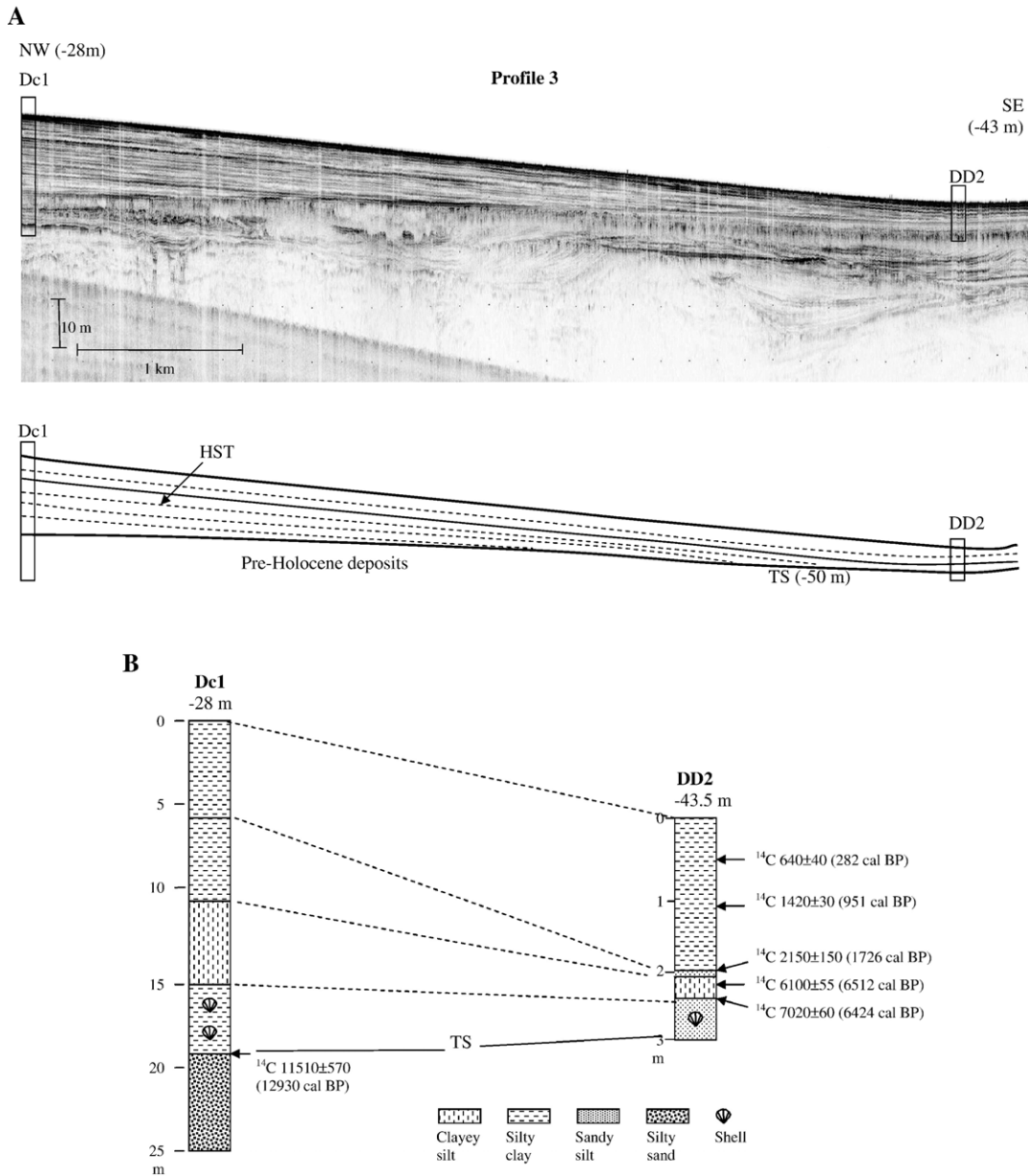


Fig. 6. (A) Seismic profile 3, showing two units of the clinoform within the HST deposits. (B) Core correlations between DC1 and DD2 show the starting age of the HST deposits and the depositional hiatus inside the HST. Location of profile and cores is shown in Fig. 3.

after sea level reached its mid-Holocene Highstand. Core DD2 and PC-6 suggest the top unit in HST was formed in recent 2000 yrs. The timing and significance of the differentiated HST layers is discussed below.

4.3. Mud wedge isopach and sediment budget

Fig. 12 shows the total thickness of Yangtze-derived sediment accumulated above the MFS, i.e. younger than ~7 ka BP. We have divided this extensive deposit into two

sub-areas: Area 1 represents the Yangtze Delta System (YDS), which includes the subaerial delta plain and estuary, and also the adjacent subaqueous delta. Area 2 is the Zhejiang–Fujian Mud Wedge (ZFMW) which represents the distal part of the Yangtze-derived mud deposits transported by the ZFCC south of Hangzhou Bay.

Total sediment volume in the delta plain and estuary of the YDS is $5 \times 10^{11} \text{ m}^3$, or about $8 \times 10^{11} \text{ t}$ (Li et al., 2003), assuming a dry bulk density of 1.6 g cm^{-3} (Hu and Yang, 1983). The volume of the subaqueous delta

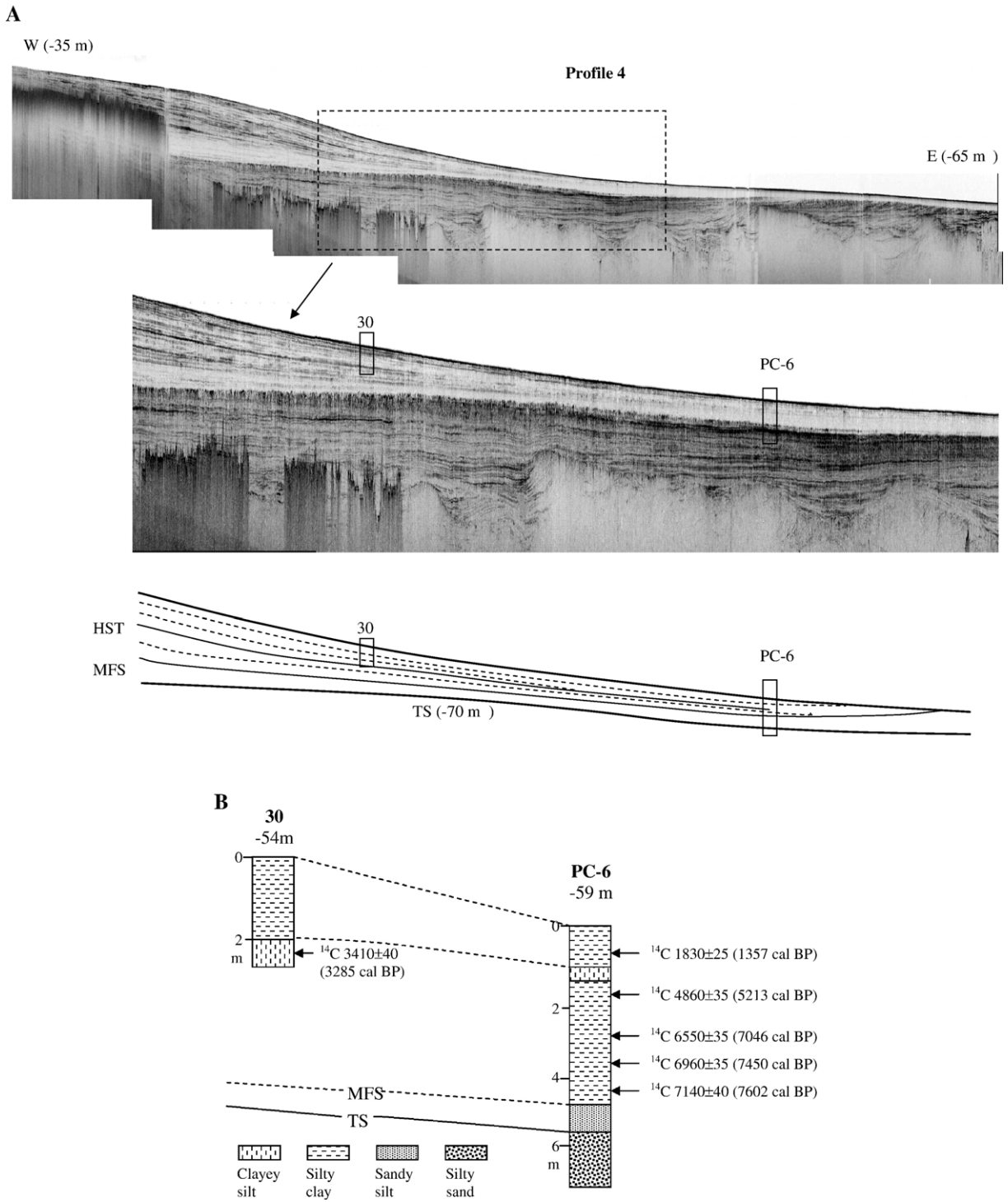


Fig. 7. (A) Seismic profile 4 and an enlargement, showing TS, MFS and HST. (B) Core correlations between 30 and PC-6, show the starting age of the HST deposits and the depositional hiatus inside the HST. Location of profile and cores is shown in Fig. 3.

off the river mouth and in Hangzhou Bay has been estimated as $3 \times 10^{11} \text{ m}^3$ (Chen and Stanley, 1993; Chen et al., 2000), but the dry bulk density of the subaqueous

deposits is presumably much less than the more compact subaerially deposited sediments. We assume an average dry bulk density of the subaqueous deltaic deposits and

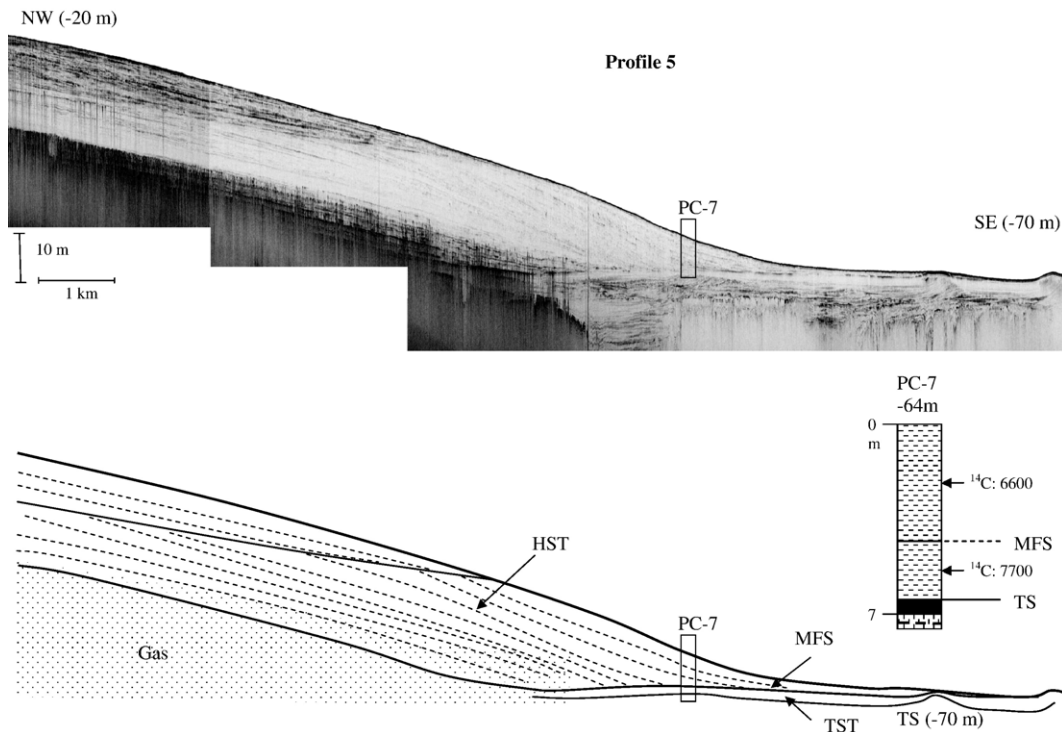


Fig. 8. Seismic profile 5 show TS, MFS and HST. The inserted core PC-7 show the relative age of the HST. Location of profile and core is shown in Fig. 3.

mud wedge from our core analysis to be $\sim 1.2 \text{ g cm}^{-3}$ which is close to Zhao et al.'s (1991) results in the Yellow Sea. Thus the subaqueous deposit in YDS could have $3.6 \times 10^{11} \text{ t}$ of sediment. Thus, during the Holocene the total sediments have accumulated in the delta plain, estuary, and subaqueous delta, in north of the latitude 30°N , is about $11.6 \times 10^{11} \text{ t}$. Total volume of the alongshore distal clinoform in the ZFMW (Area 2) is estimated to be about $4.5 \times 10^{11} \text{ m}^3$, or corresponds to $5.4 \times 10^{11} \text{ t}$ of sediment.

Overall, therefore, the Yangtze River has delivered about $1.7 \times 10^{12} \text{ t}$ of material over the last 7000 yrs, an average of $2.4 \times 10^8 \text{ t yr}^{-1}$, which is same as the estimate of Saito et al. (2001). Nearly 47% of the Yangtze-derived sediment has accumulated in the delta and estuary system, and about 21% deposited in the nearshore subaqueous deltaic systems (Area 1 in Fig. 12). The remaining 32% is believed to have been re-suspended and transported southward and accumulated at ZFMW in the inner shelf along the coasts (Area 2). Interestingly, the ratio of the southward transport is larger than Shen's (2001) estimate of 11%, but nearly identical to the 30% estimate of Milliman et al. (1985). Previous studies in the middle shelf of East China Sea also show that very little of the Yangtze sediment

presently escapes the shelf to the deep sea (Shen, 2001; Hu and Yang, 2001).

5. Development of the Yangtze-derived clinoform

The Yangtze releases the fifth largest volume globally of fresh water and fourth largest volume globally of suspended sediment to the East China Sea (Milliman and Meade, 1983; Milliman and Syvitski, 1992). However, the hydrologic data have been collected at the Datong Hydrologic Station, more than 600 km upstream from the river mouth (Fig. 2). How much of the Yangtze sediment actually reaches the East China Sea is uncertain.

Some attempts have already been carried out to calculate how much is deposited in the Yangtze delta and adjacent estuaries, how much in the adjacent subaqueous delta, and how much has been transported farther south. For instance, Chen et al. (1988) estimated that about 50% of the suspended materials settle in the lower 600 km of the river and in its estuary, the rest being dispersed into the East China Sea. Detailed calculations made by Shen (2001) indicate 31% of the modern Yangtze-derived sediment accumulates in the estuary, 40% is deposited at the Hangzhou Bay and the

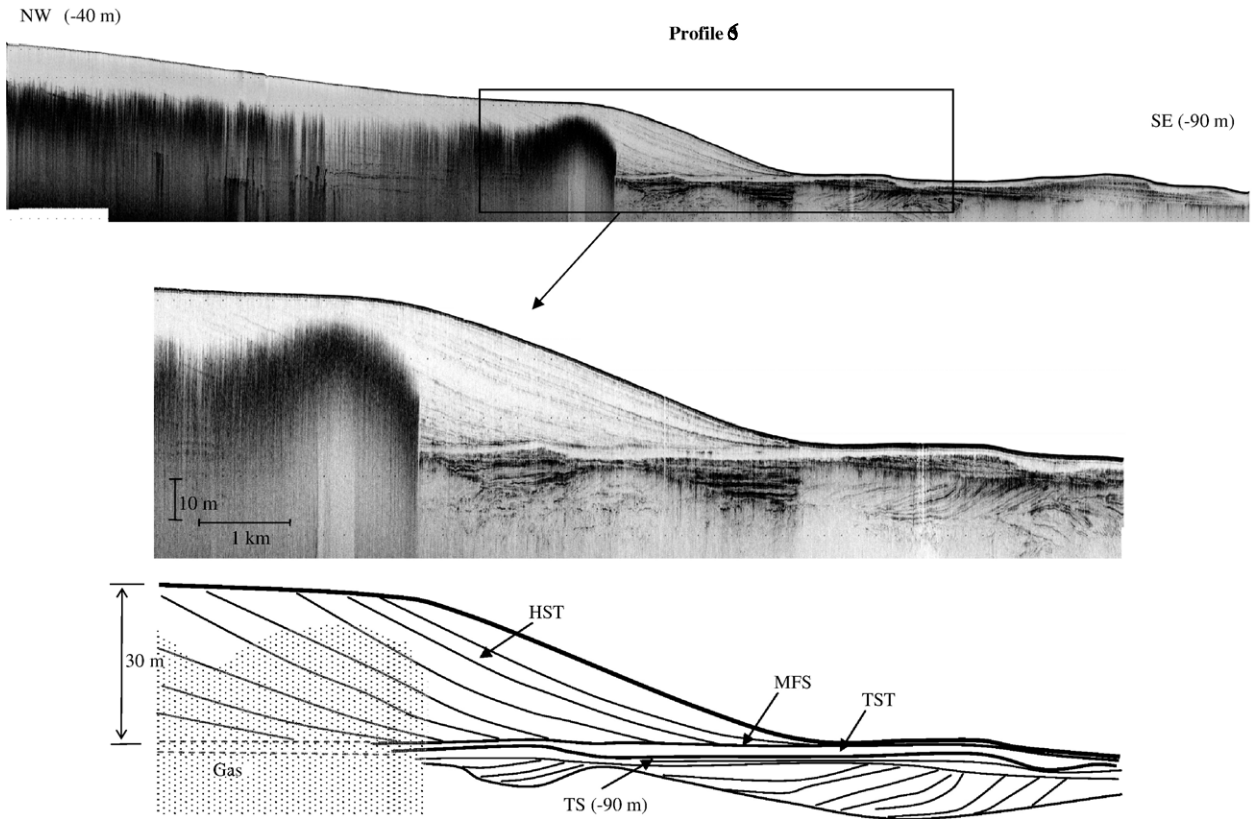


Fig. 9. Seismic profile 6 show TS, MFS and HST. Location of profile and cores is shown in Fig. 3.

surrounding areas, and only 11% is transported farther southward along the Zhejiang–Fujian coastal zone. Extensive cores collected in the deltaic plain and offshore suggest that the Yangtze River has delivered $1.18\text{--}3.54 \times 10^8$ t sediment to the ocean annually since the Last Glacial Maximum (Li et al., 2003).

The data presented in this paper allow us to map the distribution and thickness of the Yangtze-derived mud in the inner shelf of the East China Sea more quantitatively (Fig. 12). And based on these results, we can discuss the significant role of the postglacial sea-

level rise, the mechanism for trapping the mud in coastal waters, and other possible (local) sources of sediment.

5.1. Postglacial sea-level rise and the transgressive surface

Most modern deltas began to form as the postglacial sea-level rise decelerated in the mid-Holocene (Stanley and Warne, 1994). Many modern subaqueous clinoforms overlie a transgressive layer –60 m below the

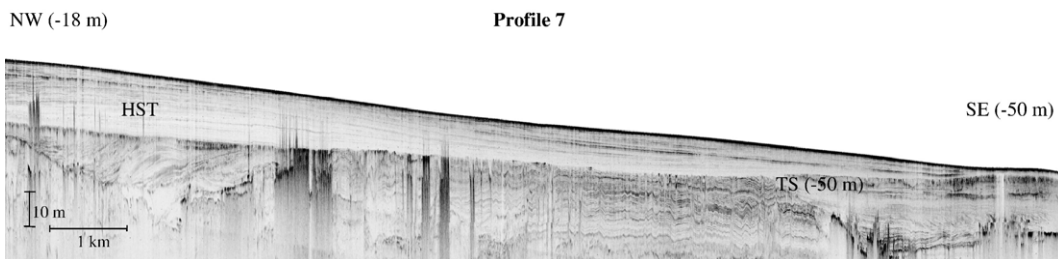


Fig. 10. Seismic profile 7 in coastal waters, showing TS and HST, but no TST and MFS. Location of profile and cores is shown in Fig. 3.

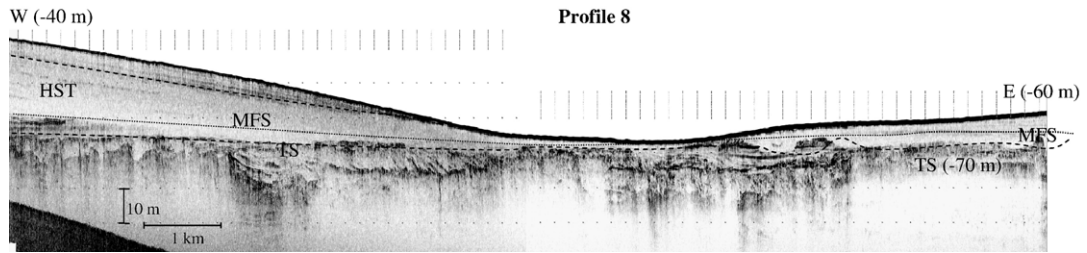


Fig. 11. Seismic profile 8 located in northwest Taiwan Strait, the southernmost line in our study area, which defines the south boundary of the Yangtze-derived mud.

present sea level, regarding for example, the Amazon (Nittrouer et al., 1996), the Yellow (Liu et al., 2002, 2004), the Ganges–Brahmaputra (Kuehl et al., 1997;

Goodbred and Kuehl, 2000), the Yangtze (Chen et al., 2000), the Ebro (Diaz et al., 1996) and the Indus (Prins and Postma, 2000).

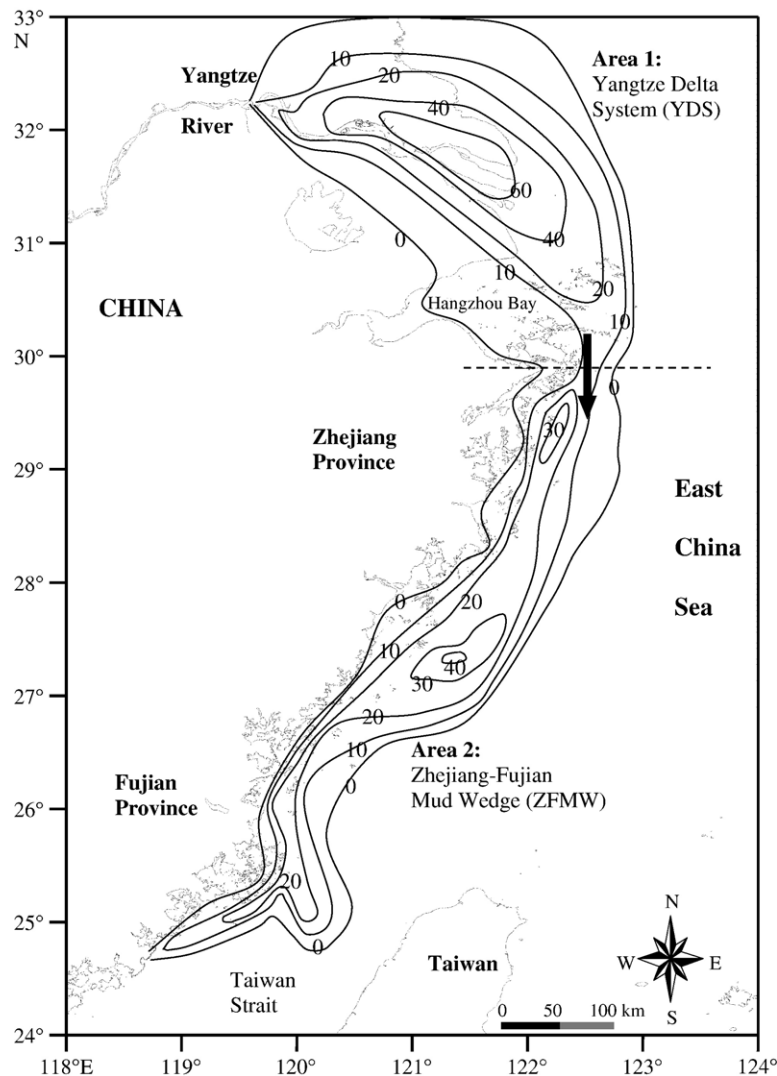


Fig. 12. Isopach map of the Yangtze-derived sediment deposited over the last 7000 yrs. Area 1 is based largely on many cores collected and analyzed by Chen and Stanley (1993), Li et al. (2000, 2001, 2002, 2003). Area 2 is delineated primarily from the seismic data presented in this paper. The southernmost boundary is determined partly on cores collected from the Taiwan Strait (Lan et al., 1993).

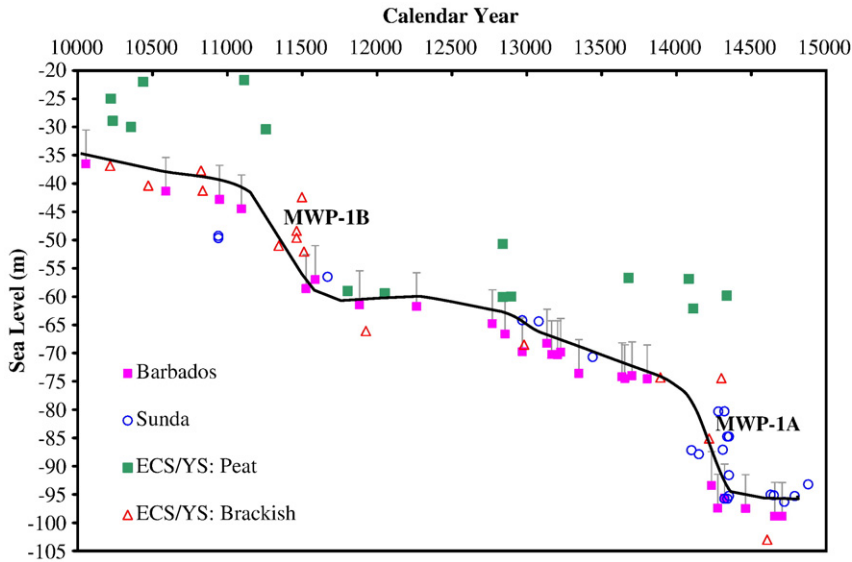


Fig. 13. Postglacial rapid sea-level rise of MWP-1A and 1B (after Liu and Milliman, 2004).

The postglacial sea-level rise provides a large accommodation space for river-derived sediment to fill (Christie-Blick and Driscoll, 1995; Driscoll and Karner, 1999). Most of our seismic profiles show that a prominent transgressive surface (TS) beneath the clinof orm deposits ranging from 90 to 50 m below sea level. For instance, the TS depth in profile 1 is -58 m, whereas in profiles 2, 3 and 7 it is -50 m and -70 m in profiles 4, 5 and 8, and -90 m in profile 6. The TS suggests rapid sea-level rise, which flooded previous deposits, truncated the channel-filled strata, and left an unconformity (and therefore a prominent acoustic reflector), and furthermore created the accommodation space for the later sediment accumulation.

The local relative sea-level history becomes a key to understand this transgression and subsequent HST deposits. Recent efforts have been made to constrain the timing and depth range of the western Pacific postglacial sea-level history using the extensive sea-level indicators collected from the Sunda, East China Sea and Yellow Sea shelves (Hanebuth et al., 2000; Liu and Milliman, 2004). The revised sea-level curve (Fig. 13) shows a rapid sea-level rise from -96 m to -80 m during Meltwater Pulse-1A (MWP-1A) during the period 14.3 ka – 14.1 ka BP. The next rapid sea-level rise from -60 m to -40 m (MWP-1B) occurred between 11.5 ka and 11.2 ka BP in the East China Sea and Yellow Sea (Liu and Milliman, 2004). In the 2500-year interval between MWP-1A and 1B, sea level rose slowly from -80 m to -60 m, and may have even retreated slightly during the Younger Dryas (YD) cooling event around 12 ka BP.

From the seismic records and sea-level history, the deeper TS at -70 to -90 m (profiles 4, 5, 6, 8) are

apparently associated with the rapid MWP-1A event and subsequent slow rise. The shallower TS from -58 m to -50 m (line 1, 2, 3, 7) may be related to MWP-1B. Thus, in our study area, the inner shelf of East China Sea has experienced at least two rapid sea-level rises (MWP-1A and 1B), punctuated by a long-term stillstand.

The most intriguing observation is that a thin TST deposit is seen only in those profiles with the deeper TS, for example, profiles 4, 5, 6 and 8, where the TS depth is deeper than -70 m (after the MWP-1A transgression). For those profiles with shallower TS, i.e. profiles 1, 2, 3 and 7, there is no TST. In other words, there no TST apparently developed after the MWP-1B transgression. Generally speaking, as the rate of relative sea-level rise increases, distal parts of the shelf become sediment-starved because the locus of sedimentation moves quickly landward. The existence of the TST in the deeper basin might be related to two things: 1) During the slow rise of sea-level between MWP-1A and 1B, the East China Sea shelf may have received mud input, as suggested by the transparent nature of the TST. Previous studies have shown that the palaeo-Yangtze River probably discharged into the East China Sea to the east of the Hangzhou bay (30° N, 123° E) when sea level was at ~ 60 m (Chen et al., 1986; Li and Wang, 1998; Li et al., 2000) (Fig. 14a). If correct, the Yangtze sediment load at that time must have been lower than that at present since we see no evidence of wide-spread early-Holocene deltaic deposits in the mid-East China Sea shelf (Liu, 1997; Berne et al., 2002); 2) The slow sea-level rise after MWP-1A (or possible falling during YD) might also help accumulate a thin retrograding/aggradational parasequence.

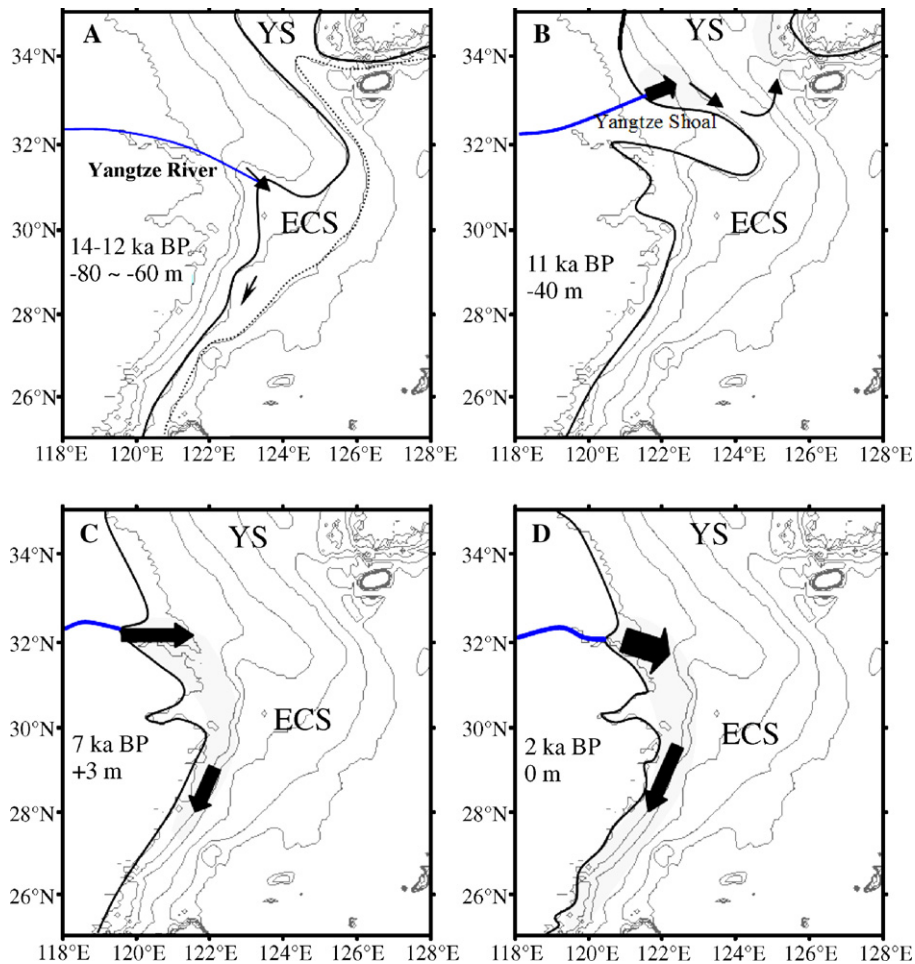


Fig. 14. Evolution of the Yangtze River and its sediment dispersal in the Yellow Sea and East China Sea in the last 14 k yrs. The shading parts represent the Yangtze-derived mud deposits on the shelf.

In contrast, there is no TST deposit after MWP-1B sea-level rise from -60 to -40 m. As the rate of relative sea-level rise increased, the sediment starvation moved to landward position, and the entire inner shelf of the East China Sea may have been sediment-starved. With the rapid sea-level rise, in the early Holocene, the palaeo-Yangtze had reportedly shifted into the south Yellow Sea (Fig. 14b) (Huang and Shen, 1987; Li et al., 2000, 2001, 2002). Due to the presence of the prominent Yangtze Shoal extending eastward from the modern Yangtze River mouth, the Yangtze-derived sediment might not have been able to be transported to the south between MWP-1B and the middle Holocene sea-level highstand (Zhao, 1984; Xia and Liu, 2001). Combined with the rapid increase in accommodation space the Yangtze River's early-to-middle Holocene deltaic deposits apparently were concentrated inland, west and north of the present Yangtze river mouth (Li et al., 2000, 2001), not along the south East China Sea shelf.

As sea-level rise continued, the Yangtze River retreated further westward from the Yellow Sea to the Jiangsu coast, north of the modern river mouth. When the sea level reached its maximum at the middle Holocene high stand at 7500–7000 yrs, a huge estuary was formed (Fig. 14c) in the present Yangtze delta area (Chen et al., 1988; Li et al., 2002). Afterwards delta progradation occurred from about 6000 to 7000 yrs BP, with an average annual progradation rate of the delta front of about 50 m, over the last 5000 yrs (Hori et al., 2001, 2002). This is also the time period when the clinof orm mud wedge began to deposit in the inner shelf of the East China Sea (Fig. 14c).

The progradation rate of the Yangtze delta, however, increased abruptly at ca. 2000 yrs BP, going from 38 to 80 m/yr (Hori et al., 2001). The possible causes for this active progradation could have been an increase in sediment production in the drainage basin due to widespread human interference and/or decrease in deposition in the middle reaches related to the channel stability caused by

human activity and climatic cooling after the mid-Holocene (Saito et al., 2001; Hori et al., 2001, 2002; Xiao et al., 2004), or related to the middle to late Holocene sea level fall and then regressive processes (Li et al., 2002, 2003). This shift can be seen in most of our profiles and core stratigraphies. The sequence and inner structure of the HST in the Zhejiang–Fujian mud wedge are consistent with the observation in the Yangtze delta plain by seismic profiling and coring (Wang et al., 2007–this volume).

5.2. Alongshore dispersal of Yangtze sediment

Historically, the Yangtze-derived sediment began to be transported southward after the middle Holocene sea-level highstand, around 7 ka BP. In addition to sea-level rise and delta formation, the other driving force was the China Coastal Currents system. With the postglacial sea-level rise and global warming, the main flow of the Kuroshio Current began to re-enter the Okinawa Trough at 7.3 ka BP (Jian et al., 2000). In response, the YSWC and Chinese coastal currents (JCC and ZFCC) began to flow out of the East China Sea, thereby playing a critical role transporting the Yangtze-derived sediment to the south. This matches well of the ^{14}C dating (~ 7 ka BP) in the bottom of the HST (Figs. 6B, 7B, 8).

Suspended matter, temperature and salinity surveys conducted in the northwestern East China Sea show that near-bottom concentrations of suspended matter are much higher during the winter than the summer, due in large part to winter storms and the well-mixed water column (Milliman et al., 1985, 1989; Yang et al., 1992; Guo et al., 2002, 2003). Actually, the isopach map shows most of the Yangtze-derived sediment accumulates west of 123°

E (Fig. 12). Hu (1984) suggested that sediment distribution is associated with the coastal upwelling system. In winter, monsoon-driven coastal currents flow southward and cause downwelling in nearshore, while the northward Taiwan Warm Current causes upwelling. With the two vertical circulation cells (downwelling near the coast and upwelling offshore) fine sediment transport is constrained under the upwelling (compare Figs. 12 and 15).

5.3. Other sediment sources — local small rivers

Like in other large coastal mud wedges derived extensively from a single sediment source, e.g., the Amazon (Allison et al., 2000), Po (Cattaneo et al., 2003), and Yellow (Liu et al., 2004) rivers, smaller coastal rivers may have local or even regional importance. Along the Zhejiang and Fujian Provinces, there are three small mountainous rivers, Qiantang, Ou, and Min rivers. Together, they could deliver an average $\sim 18 \times 10^6$ t sediment annually to the coast (Qin et al., 1987; Zhu, 1993), only $\sim 4\%$ of the present Yangtze's annual sediment load. Another possible source is the hyperpycnal flows from Taiwan rivers as indicated by recent study by Milliman and Kao (2005). To define the quantitative importance of these rivers, however, will require further research, involving both geochemical tracers (to determine provenance) and physical oceanographic data (to determine transport mechanisms).

6. Conclusions

The extensive alongshore mud wedge, extending down to Taiwan Strait, represents the southward transport of Yangtze-derived sediment during the middle to late-Holocene HST by the Zhejiang–Fujian Coastal Current. This Holocene mud wedge directly overlies a thin and flat layer separated with a regional downlap surface that marks a maximum landward shift of the shoreline at the end of the rapid rises of post-glacial sea level, MWP-1A and 1B. Above this unit, there is an extensive clinoform deposit, with a depocenter (~ 40 m thick) located between the 20–30 m isobaths in the north, progressively thinning offshore, and diminishing at water depths from 60 to 70 m and to the south.

Total sediment volume of the clinoform in the Zhejiang–Fujian mud wedge is estimated to be about 4.5×10^{11} m³, which represents about 32% the total Yangtze-derived mud to the sea; the rest is believed to have been trapped in the Yangtze estuary and deltaic system. AMS ^{14}C dates suggest that most of this mud has been transported southward in the past 7000 yrs BP by the newly formed Chinese Coastal Current after sea level reached its mid-Holocene highstand. This would

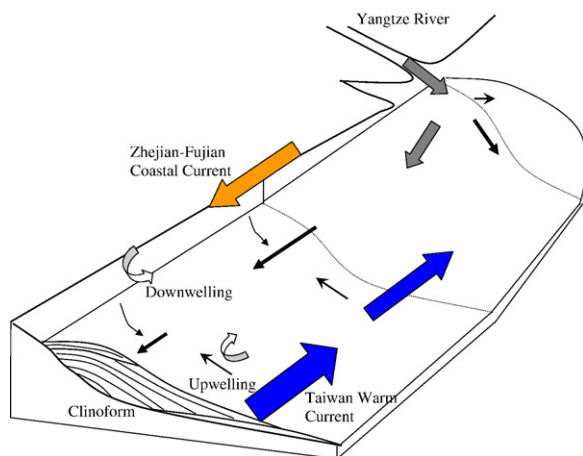


Fig. 15. Sedimentary and oceanographic processes affecting the sediment dispersal at both across-and along shelf directions, and the formation of the clinoform.

equate to an annual sediment load of 2.4×10^8 t, which is about half the current annual Yangtze sediment discharge. The increased sediment discharge and the seaward progradation rate in the last 2000 yrs reflect the stabilization of the recent sea level and the forcing from climatic and anthropogenic changes.

The southward elongation of the shore-parallel mud wedge has been facilitated by the downwelling ZFCC and upwelling Taiwan Warm Current in the middle shelf, which also have helped block the escape of any Yangtze-derived sediment to the Okinawa Trough.

Acknowledgments

Many thanks to the crews of RV Goldenstar II and many Chinese and American colleagues for their help on the cruise and post-cruise data processing. Financial support for this joint research came from the International Office of the U.S. NSF, China NSF, ONR, and internal funding from IOCAS and NCSU. The authors thank S.W. Lin, C.S. Liu and J.K. Chiu from National Taiwan Univ., who helped define the southern boundary of the mud wedge in Taiwan Strait. We thank D.J. DeMaster for his helpful comments on an earlier version of this paper. We also thank Prof. Z. Chen and an anonymous reviewer for significantly improving the manuscript.

References

- Allison, M.A., Lee, M.T., Ogston, A.S., Aller, R.C., 2000. Origin of Amazon mudbanks along the northeastern coast of South America. *Marine Geology* 163 (1–4), 241–256.
- Bartek, L.R., Wellner, R.W., 1995. Do equilibrium conditions exist during sediment transport studies? An example from the East China Sea. *Geo-Marine Letters* 15, 23–29.
- Beardsley, R.C., Limeburner, R., Yu, H., Cannon, G.A., 1985. Discharge of the Changjiang (Yangtze River) into the East China Sea. *Continental Shelf Research* 4 (1–2), 57–76.
- Berne, S., Vagner, P., Guichard, F., Lericolais, G., Liu, Z., Trentesaux, A., Yin, P., Yi, H.L., 2002. Pleistocene forced regressions and tidal sand ridges in the East China Sea. *Marine Geology* 188 (3–4), 293–315.
- Butenko, J., Milliman, J.D., Ye, Y., 1985. Geomorphology, shallow structure, and geological hazards in the East China Sea. *Continental Shelf Research* 4 (1–2), 121–141.
- Cai, W.-J., Dai, M., 2004. Comment on “Enhanced Open Ocean Storage of CO₂ from Shelf Sea Pumping”. *Science* 306 (5701), 1477.
- Cattaneo, A., Correggiari, A., Langone, L., Trincardi, F., 2003. The late-Holocene Gargano subaqueous delta, Adriatic shelf: sediment pathways and supply fluctuations. *Marine Geology* 193 (1–2), 61–91.
- Chen, Z., Stanley, D.J., 1993. Yangtze delta, eastern China: 2. Late Quaternary subsidence and deformation. *Marine Geology* 112 (1–4), 13–21.
- Chen, C.T.A., Wang, S.L., 1999a. Carbon, alkalinity and nutrient budgets on the East China Sea continental shelf. *Journal of Geophysical Research, C: Oceans* 104 (9), 20,675–20,686.
- Chen, Z.Y., Wang, Z.H., 1999b. Yangtze Delta, China: Taihu lake-level variation since the 1950s, response to sea-level rise and human impact. *Environmental Geology* 37 (4), 333–339.
- Chen, Z.Y., Zhou, C.Z., Yang, W.D., Wu, Z.G., 1986. Submarine topography and sediments off modern Yangtze River. *Donghai Marine Science* 4 (4), 28–37 (in Chinese, with English Summary).
- Chen, J.Y., Shen, H.T., Yun, C.X., 1988. Process of Dynamics and Geomorphology of the Changjiang Estuary. Shanghai Science and Technology Press, Shanghai. 454 pp.
- Chen, Z., Chen, Z.L., Zhang, W.G., 1997. Quaternary stratigraphy and trace-element indices of the Yangtze Delta, Eastern China, with special reference to marine transgressions. *Quaternary Research* 47 (2), 181–191.
- Chen, Z., Song, B., Wang, Z., Cai, Y., 2000. Late Quaternary evolution of the sub-aqueous Yangtze Delta, China: sedimentation, stratigraphy, palynology, and deformation. *Marine Geology* 162 (2–4), 423–441.
- Chen, Z., Li, J., Shen, H., Zhanghua, W., 2001. Yangtze River of China: historical analysis of discharge variability and sediment flux. *Geomorphology* 41 (2–3), 77–91.
- Chen, C.-T.A., Liu, K.-K., MacDonald, R.W., 2003a. Continental margin exchanges. In: Fasham, M.J.R. (Ed.), *Ocean Biogeochemistry — The Role of the Ocean Carbon Cycle in Global Change*. IGBP Book Series. Springer, pp. 53–97.
- Chen, Z., Saito, Y., Hori, K., Zhao, Y., Kitamura, A., 2003b. Early Holocene mud-ridge formation in the Yangtze offshore, China: a tidal-controlled estuarine pattern and sea-level implications. *Marine Geology* 198 (3–4), 245–257.
- Chen, Z., Saito, Y., Kanai, Y., Wei, T., Li, L., Yao, H., Wang, Z., 2004. Low concentration of heavy metals in the Yangtze estuarine sediments, China: a diluting setting. *Estuarine, Coastal and Shelf Science* 60 (1), 91–100.
- Christie-Blick, N., Driscoll, N.W., 1995. Sequence stratigraphy. *Annual Review of Earth and Planetary Sciences* 23, 451–478.
- Dagg, M., Benner, R., Lohrenz, S., Lawrence, D., 2004. Transformation of dissolved and particulate materials on continental shelves influenced by large rivers: plume processes. *Continental Shelf Research* 24 (7–8), 833–858.
- DeMaster, D.J., McKee, B.A., Nittrouer, C.A., Qian, J., Cheng, G., 1985. Rates of sediment accumulation and particle reworking based on radiochemical measurements from continental shelf deposits in the East China Sea. *Continental Shelf Research* 4 (1–2), 143–158.
- Diaz, J., Palanques, A., Nelson, C.H., Guillen, J., 1996. Morpho-structure and sedimentology of the Holocene Ebro prodelta mud belt (northwestern Mediterranean Sea). *Continental Shelf Research* 16 (4), 435–456.
- Driscoll, N.W., Kerner, G.D., 1999. Three-dimensional quantitative modeling of clinoform development. *Marine Geology* 154 (1–4), 383–398.
- Goodbred, S.L., Kuehl, S.A., 2000. The significance of large sediment supply, active tectonism, and eustasy on margin sequence development: late Quaternary stratigraphy and evolution of the Ganges–Brahmaputra delta. *Sedimentary Geology* 133 (3–4), 227–248.
- Guo, Z.G., Yang, Z.S., Zhang, D.Q., Fan, D.J., Lei, K., 2002. Seasonal distribution of suspended matter in the northern East China Sea and barrier effect of current circulation on its transport. *Acta Oceanologica Sinica* 24 (5), 71–80 (in Chinese, with English Summary).
- Guo, Z.G., Yang, Z.S., Fan, D.J., J.P.Y., 2003. Seasonal sedimentary effect on the Changjiang estuary mud area. *Acta Geographica Sinica* 58 (4), 591–597 (in Chinese, with English Summary).

- Hanebuth, T., Stattegger, K., Grootes, P.M., 2000. Rapid flooding of the Sunda Shelf: a late-glacial sea-level record. *Science* 288 (5468), 1033–1035.
- Hori, K., Cheng, X., Wang, P., Sato, Y., Li, C., Saito, Y., Zhao, Q., 2001. Sedimentary facies and Holocene progradation rates of the Changjiang (Yangtze) delta, China. *Geomorphology* 41 (2), 233–248.
- Hori, K., Saito, Y., Zhao, Q., Wang, P., 2002. Architecture and evolution of the tide-dominated Changjiang (Yangtze) River delta, China. *Sedimentary Geology* 146 (3–4), 249–264.
- Hu, D.X., 1984. Upwelling and sedimentation dynamics: 1. the role of upwelling in sedimentation in the Huanghai Sea and East China Sea: a description of general features. *Chinese Journal of Oceanologia and Limnologia* 2 (1), 12–19 (in Chinese, with English Summary).
- Hu, G.T., Yang, W.Y., 1983. *Engineering Geology*. China Geology Press, Beijing. 26 pp. (in Chinese).
- Hu, D.X., Yang, Z.S., 2001. *Key Processes of the East China Sea Flux*. China Ocean Press, Beijing. 204 pp. (in Chinese, with English Summary).
- Huang, H.Z., Shen, B.P., 1987. Origin of the hyperopic deposits in the Holocene Changjiang subaqueous delta. *Marine Geology & Quaternary Geology* 7 (4), 57–65 (in Chinese, with English Summary).
- Huh, C.A., Su, C.C., 1999. Sedimentation dynamics in the East China Sea elucidated from ^{210}Pb , ^{137}Cs and $^{239,240}\text{Pu}$. *Marine Geology* 160 (1–2), 183–196.
- Jian, Z., Wang, P., Saito, Y., Wang, J., Pflaumann, U., Oba, T., Cheng, X., 2000. Holocene variability of the Kuroshio Current in the Okinawa Trough, northwestern Pacific Ocean. *Earth and Planetary Science Letters* 184 (1), 305–319.
- Kuehl, S.A., Levy, B.M., Moore, W.S., Allison, M.A., 1997. Subaqueous delta of the Ganges–Brahmaputra river system. *Marine Geology* 144 (1–3), 81–96.
- Lan, D.Z., Zhang, W.L., Chen, C.H., Xie, Z.T., Yu, Y.F., Cai, F., 1993. Transgressions and the sea-level changes of the western Taiwan Strait since the Late Pleistocene. *Acta Oceanologica Sinica* 12 (4), 617–627.
- Lee, H.-J., Chao, S.-Y., 2003. A climatological description of circulation in and around the East China Sea. *Deep-Sea Research, Part II: Topical Studies in Oceanography* 50 (6–7), 1065–1084.
- Li, C.X., Wang, P.X., 1998. *Late Quaternary Stratigraphy of the Yangtze Delta*. China Science Press, Beijing. 222 pp. (in Chinese).
- Li, C.X., Ming, Q.B., Sun, H.P., 1986. Holocene strata and transgression of southern Yangtze delta plain. *Chinese Science Bulletin* 21, 1650–1653.
- Li, C., Chen, Q., Zhang, J., Yang, S., Fan, D., 2000. Stratigraphy and paleoenvironmental changes in the Yangtze Delta during the Late Quaternary. *Journal of Asian Earth Sciences* 18 (4), 453–469.
- Li, C.X., Deng, B., Zhang, J.Q., Fan, D.D., 2001. Holocene regression and the tidal radial sand ridge system formation in the Jiangsu coastal zone, east China. *Marine Geology* 173 (1–4), 97–120.
- Li, C., Wang, P., Sun, H., Zhang, J., Fan, D., Deng, B., 2002. Late Quaternary incised-valley fill of the Yangtze delta (China): its stratigraphic framework and evolution. *Sedimentary Geology* 152 (1–2), 133–158.
- Li, B.H., Li, C.X., Shen, H.T., 2003. A preliminary study on sediment flux in the Changjiang Delta during the postglacial period. *Science in China, Series D: Earth Sciences* 46 (7), 743–752.
- Lin, S., Hsieh, I.-J., Huang, K.-M., Wang, C.-H., 2002. Influence of the Yangtze River and grain size on the spatial variations of heavy metals and organic carbon in the East China Sea continental shelf sediments. *Chemical Geology* 182 (2–4), 377–394.
- Liu, Z.X., 1997. Yangtze Shoal — a modern tidal sand sheet in the northwestern part of the East China Sea. *Marine Geology* 137 (3–4), 321–330.
- Liu, Z.-X., Berne, S., Saito, Y., Lericolais, G., Marsset, T., 2000. Quaternary seismic stratigraphy and paleoenvironments on the continental shelf of the East China Sea. *Journal of Asian Earth Sciences* 18 (4), 441–452.
- Liu, K.-K., Peng, T.-H., Shaw, P.-T., Shiah, F.-K., 2003. Circulation and biogeochemical processes in the East China Sea and the vicinity of Taiwan: an overview and a brief synthesis. *Deep-Sea Research, Part II: Topical Studies in Oceanography* 50 (6–7), 1055–1064.
- Liu, J.P., Milliman, J.D., Gao, S., 2002. The Shandong mud wedge and post-glacial sediment accumulation in the Yellow Sea. *Geo-Marine Letters* 21 (4), 212–218.
- Liu, J.P., Milliman, J.D., 2004. Reconsidering melt-water pulses 1A and 1B: global impacts of rapid sea-level rise. *Journal of Ocean University of China* 3 (3), 183–190.
- Liu, J.P., Milliman, J.D., Gao, S., Cheng, P., 2004. Holocene development of the Yellow River's subaqueous delta, North Yellow Sea. *Marine Geology* 209 (1–4), 45–67.
- McKee, B.A., Nittrouer, C.A., DeMaster, D.J., 1983. Concepts of sediment deposition and accumulation applied to the continental shelf near the mouth of the Yangtze River. *Geology* 11 (11), 631–633.
- McKee, B.A., Aller, R.C., Allison, M.A., Bianchi, T.S., Kineke, G.C., 2004. Transport and transformation of dissolved and particulate materials on continental margins influenced by major rivers: benthic boundary layer and seabed processes. *Continental Shelf Research* 24 (7–8), 899–926.
- Meade, R.H., 1996. River-sediment inputs to major deltas. In: Milliman, J., Haq, B. (Eds.), *Sea-Level Rise and Coastal Subsidence*. Kluwer, London, pp. 63–85.
- Milliman, J.D., Kao, S.J., 2005. Hyperpycnal discharge of fluvial sediment to the ocean: impact of Super-Typhoon Herb (1996) on Taiwanese rivers. *Journal of Geology* 113, 503–516.
- Milliman, J.D., Meade, R.H., 1983. World-wide delivery of sediment to the oceans. *Journal of Geology* 91 (1), 1–21.
- Milliman, J.D., Syvitski, J.P.M., 1992. Geomorphic/tectonic control of sediment discharge to the ocean: the importance of small mountainous rivers. *Journal of Geology* 100 (5), 525–544.
- Milliman, J.D., Shen, H.T., Yang, Z.S., Meade, R.H., 1985. Transport and deposition of river sediment in the Changjiang estuary and adjacent continental shelf. *Continental Shelf Research* 4 (1–2), 37–45.
- Milliman, J.D., Qin, Y.S., Park, Y., 1989. Sediment and sedimentary processes in the Yellow and East China Seas. In: Taira, A., Masuda, F. (Eds.), *Sedimentary Facies in the Active Plate Margin*. Terra Scientific Publishing Company, Tokyo, pp. 233–249.
- Nittrouer, C.A., DeMaster, D.J., McKee, B.A., 1984. Fine-scale stratigraphy in proximal and distal deposits of sediment dispersal systems in the East China Sea. *Marine Geology* 61 (1), 13–24.
- Nittrouer, C.A., Kuehl, S.A., Figueiredo, A.G., Allison, M.A., Sommerfield, C.K., Rine, J.M., Faria, L.E.C., Silveira, O.M., 1996. The geological record preserved by Amazon shelf sedimentation. *Continental Shelf Research* 16 (5–6), 817–841.
- Prins, M.A., Postma, G., 2000. Effects of climate, sea level, and tectonics unraveled for last deglaciation turbidite records of the Arabian Sea. *Geology* 28 (4), 375–378.
- Qin, Y.S., 1979. A study on sediment and mineral compositions of the sea floor of the East China Sea. *Oceanic Selections* 2 (2), 130–142.
- Qin, Y.S., Zhao, Y.Y., Chen, L.R., Zhao, S.L., 1987. *Geology of the East China Sea*. China Science Press, Beijing. 290 pp.
- Saito, Y., Katayama, H., Ikehara, K., Kato, Y., Matsumoto, E., Oguri, K., Oda, M., Yumoto, M., 1998. Transgressive and highstand systems tracts and post-glacial transgression, the East China Sea. *Sedimentary Geology* 122 (1–4), 217–232.

- Saito, Y., Yang, Z., Hori, K., 2001. The Huanghe (Yellow River) and Changjiang (Yangtze River) deltas: a review on their characteristics, evolution and sediment discharge during the Holocene. *Geomorphology* 41 (2–3), 219–231.
- Shen, H.T., 2001. Material Flux of the Changjiang Estuary. China Ocean Press, Beijing. 176 pp. (in Chinese).
- Stanley, D.J., Chen, Z., 1996. Neolithic settlement distributions as a function of sea level-controlled topography in the Yangtze delta, China. *Geology* 24 (12), 1083–1086.
- Stanley, D.J., Warne, A.G., 1994. Worldwide initiation of Holocene marine deltas by deceleration of sea-level rise. *Science* 265, 228–231.
- Stuiver, M., Burr, G.S., Hughen, K.A., Kromer, B., McCormac, G., Van Der Plicht, J., Spurk, M., Reimer, P.J., Bard, E., Beck, J.W., 1998. INTCAL98 radiocarbon age calibration, 24,000–0 cal BP. *Radiocarbon* 40 (3), 1041–1083.
- Su, C.C., Huh, C.A., 2002. ^{210}Pb , ^{137}Cs and $^{239,240}\text{Pu}$ in East China Sea sediments: sources, pathways and budgets of sediments and radionuclides. *Marine Geology* 183 (1–4), 163–178.
- Syvitski, J.P.M., Vorosmarty, C.J., Kettner, A.J., Green, P., 2005. Impact of humans on the flux of terrestrial sediment to the global coastal ocean. *Science* 308 (5720), 376–380.
- Tsunogai, S., Saito, Y., Iseki, K., Kusakabe, M., 2003. Biogeochemical cycles in the East China Sea: MASFLEX program. *Deep-Sea Research, Part II: Topical Studies in Oceanography* 50 (2), 321–326.
- Wang, Z., Saito, Y., Hori, K., Kitamura, A., Chen, Z., 2005. Yangtze offshore, China: highly laminated sediments from the transition zone between subaqueous delta and the continental shelf. *Estuarine, Coastal and Shelf Science* 62 (1–2), 161–168.
- Wang, Z.H., Chen, Z.Y., Chen, J., Wei, Z.X., 2007. Seismic framework to interpret the morphological evolution of the Changjiang River mouth, China *Geomorphology* 85, 237–248 (this volume). doi: [10.1016/j.geomorph.2006.03.022](https://doi.org/10.1016/j.geomorph.2006.03.022).
- Xia, D.X., Liu, Z.X., 2001. Tracing the Changjiang River's flowing route entering the sea during the last ice age maximum. *Acta Oceanologica Sinica* 23 (5), 87–94 (in Chinese, with English Summary).
- Xiao, S.B., Li, A.C., Jiang, F.Q., Gang, L.T., Huang, P., Xu, Z.K., 2004. Mud deposit records in the inner shelf of the East China Sea since near 2000 a BP and its climate significance. *Chinese Science Bulletin* 49 (21), 2233–2238.
- Yan, Q.S., Hong, X.Q., 1987. Holocene transgression on the southern Yangtze plain. *Acta Geographica Sinica* 9 (6), 744–752 (in Chinese, with English Summary).
- Yang, H.R., Xie, Z.R., 1984. Sea-level changes along the east coast of China over the last 20000 years. *Oceanologia et Limnologia Sinica* 15 (1), 1–13 (in Chinese, with English Summary).
- Yang, Z.S., Guo, Z.G., Wang, Z.X., 1992. Basic pattern of transport of suspended matter from the Yellow Sea and East China Sea to the eastern deep seas. *Acta Oceanologica Sinica* 14 (2), 81–90 (in Chinese, with English Summary).
- Zhao, S.L., 1984. On the Quaternary Geological Problem of the Yangtze River delta region. *Marine Science* 15, 15–21 (in Chinese, with English Summary).
- Zhao, Y.Y., Li, F.Y., DeMaster, D.J., Nittrouer, C.A., Milliman, J.D., 1991. Preliminary studies on sedimentation rate and sediment flux of the South Huanghai Sea. *Oceanologia et Limnologia Sinica* 22 (1), 38–43 (in Chinese, with English Summary).
- Zhao, X.T., Tang, L.Y., Sun, C.M., Wang, S.H., 1994. Holocene climate and sea-level fluctuation of Qingfeng profile, Jianhu, Jiangsu province. *Acta Oceanologica Sinica* 16 (1), 78–88 (in Chinese, with English Summary).
- Zhu, D.Q., 1993. Chinese Water System Dictionary. Qingdao Publish House, Qingdao. 642 pp. (in Chinese).